Domination of dissociative double-electron excitation over dissociative single-electron excitation in electron collisions with NH_3

Kouichi Hosaka,[1,*] Kai Minamizaki,[1] Toshinori Tsuchida,[1] Kazufumi Yachi,[1] Takeshi Odagiri,[2] Takuro Maeda,[1] Masashi Kitajima,[1] and Noriyuki Kouchi[1]

[1]*Department of Chemistry, Tokyo Institute of Technology, Meguro-ku, Tokyo 152-8551, Japan*

[2]*Department of Materials and Life Sciences, Sophia University, Chiyoda-ku, Tokyo 102-8554, Japan*

(Received 26 September 2016; revised manuscript received 23 March 2017; published 24 July 2017)

Double-electron excitations in electron collisions with NH_3 are investigated in the range of the outer valence and inner valence excitations by means of angle-resolved electron-photon coincidence measurements. Double-electron and single-electron excitations are termed double and single excitations, respectively, in this article. It is found that the dissociative double excitation resulting in H($2p$) formation becomes more dominant over the dissociative single excitation at 100-eV incident energy as the electron scattering angle increases just from 8° to 15°. This remarkable domination is not expected from the independent particle model and strongly supports the double-excitation mechanism through the electron correlation induced by the penetration of the incident electron depth into the valence orbitals of a NH_3 molecule.

DOI: 10.1103/PhysRevA.96.012706

I. INTRODUCTION

It is of great significance to reveal the role of the electron correlation in a wide range of matter, from atoms and molecules to solids. In solids strongly correlated electron systems have been actively investigated from the aspect of fundamental interest and application to the electronics industry [1–3]. In atoms and molecules the transition from the ground state to the doubly excited state is a key issue in terms of the electron correlation since a multielectron transition is in general much more unfavorable than a single-electron transition within the independent particle model. Hence investigation of the double-excitation mechanism in a wide range of matter is an invaluable direction for research on the electron correlation.

Doubly excited states of atoms and molecules are embedded in an ionization continuum, unlike states below the ionization energy. The doubly excited state of molecules is not described as a product of the electronic and nuclear wave functions because of the superposition of electronically discrete and continuous states of molecules [4,5] and, thus, attracts much attention as a few-body correlated system, as shown below. Doubly excited molecules have a specific decay channel not seen in doubly excited atoms, that is, neutral dissociation. Taking advantage of neutral dissociation the superposition of electronically discrete and continuous states of molecules can be removed and only the doubly excited state separates. Over about the last decade, experimental efforts have been devoted to precise studies of the double excitation followed by neutral dissociation, i.e., dissociative double excitation, of diatomic molecules mediated by the absorption of a single photon [6–17] and electron collisions [18–21] in the range of excitation of valence electrons. Neutral dissociation of doubly excited molecules competes with autoionization. Dissociative double excitation should hence be investigated, as well as double excitation followed by autoionization [22–26], in order to obtain the full picture of the dynamics of few-body correlated systems.

Double excitation by the absorption of a single photon and fast electron collisions in the domain of the Born-Bethe approximation originates from the electron correlation in a target molecule since the interaction operators in both cases are expressed by a sum of single-electron operators [27]. However, double excitation by electron collisions at lower incident energies seems to be brought about in a much different way. It is hence of interest to investigate the double-excitation mechanism specific to electron collisions at low-to-moderate incident energies where the Born-Bethe approximation is not appropriate. In this respect, interesting results were recently obtained in electron collisions with not diatomic molecules but polyatomic molecules. Our group found that for H_2O [28] and NH_3 [29] electron collision at 100-eV incident energy and 8° electron scattering angle enhances dissociative double excitation versus dissociative single excitation in comparison with the absorption of a single photon. The momenta of the incident and scattered electrons are in the range of 2.2–2.7 a.u. (atomic units), which is around the upper edge of the momentum distributions of valence electrons in H_2O [30] and NH_3 [31] molecules. The interaction of 100-eV electrons with these molecules hence could not be expressed by a sum of single-electron operators, unlike the Born-Bethe approximation. As a result the double excitation by 100-eV electron collisions is not attributed to only the electron correlation in a target molecule. In the context of the electron correlation, the observed enhancement suggests that an incident electron of 100-eV kinetic energy penetrates so deeply into the valence orbitals in a target molecule that it induces a stronger electron correlation in an electron + molecule collision system than the electron correlation in a target molecule alone in the absorption of a single photon. To our knowledge, a limited number of precise calculations of the cross sections for double excitation by electron collisions at low-to-moderate incident energies have been carried out, but such investigations have been in progress [32–34]. It is hence fruitful to experimentally substantiate the suggested mechanism of double excitation through the electron correlation induced by penetration of the incident electron into the region of orbital electrons.

*hosakak@chem.titech.ac.jp

In this paper we aim to substantiate the double-excitation mechanism through an induced electron correlation mentioned above. For this purpose we measure the electron energy-loss spectra of NH_3 in coincidence with detecting the Lyman-α photons emitted by a neutral H($2p$) fragment at 100-eV incident energy and at electron scattering angles of 8° and 15°. These spectra are the cross sections $\langle d^3\sigma/dEd\Omega_e d\Omega_{ph}\rangle$ as a function of the energy loss E at given electron scattering angles. Here, $d^3\sigma/dEd\Omega_e d\Omega_{ph}$ is the differential cross section of the dissociative excitation resulting in H($2p$) formation per unit ranges of E and solid angles of scattered electrons, Ω_e, and emitted Lyman-α photons, Ω_{ph}. Brackets $\langle \dots \rangle$ indicate average cross sections with resolutions of E, Ω_e, and Ω_{ph}. We stress that the key to observing doubly excited molecules is measuring cross sections free of ionization since ionization makes a large contribution that prevents the observation of doubly excited states. The coincidence measurement is done to eliminate the contribution of ionization and to separate only the doubly excited state from superposition with the ionization continuum. It is predicted from the double-excitation mechanism through the induced electron correlation that the ratio of the differential cross section for dissociative double excitation to that for dissociative single excitation increases with an increase in the electron scattering angle, for the following reasons: (i) the ratio above seems to provide a good measure of the strength of the induced electron correlation, with a higher ratio indicating a stronger electron correlation; (ii) an electron collision at a smaller scattering angle takes place when an incident electron interacts with a target molecule in its outer region, which is referred to as a distant collision, while that at a larger scattering angle takes place when the incident electron interacts in the inner region and is referred to as a close collision; and (iii) it is natural that a close collision induces a stronger electron correlation than a distant collision does. The prediction is compared with the experimental result to substantiate the double-excitation mechanism through the electron correlation induced by penetration of the incident electron into the region of orbital electrons.

II. EXPERIMENT

The experimental apparatus was described in detail in our previous papers [35,36] and hence is summarized briefly here. A time-resolved position-sensitive detector of electrons was introduced for the angle-resolved measurement [35,36]. An incident electron beam produced in an electron monochromator was introduced into a gas cell filled with ammonia. Electrons scattered into a small solid angle were energy-dispersed by an electron energy analyzer incorporating a 50-mm-radius hemispherical deflector, and dispersed electrons were detected by a position-sensitive detector, which covers an energy-loss range of approximately 11-eV width because of the 50-eV pass energy of the energy analyzer. The resolution of the energy loss was approximately 650 meV. Vacuum ultraviolet photons emitted perpendicular to the scattering plane were detected by a microchannel plate incorporating a MgF_2 window, which provides a filter range of wavelength 115–150 nm. Signals from the photon detector are attributed to Lyman-α photons emitted by fragment H($2p$) atoms since the fluorescence spectrum measured at 100-eV electron impact on NH_3 [37] shows a dominant contribution of Lyman-α fluorescence in the wavelength range mentioned above. The electron beam current was estimated to be several nanoamperes. The ammonia pressure in the gas cell was carefully chosen so as to obtain a good linearity between the electron and photon count rates and the ammonia pressure, i.e., the ammonia pressure in the gas cell was lower than 0.03 Pa, which was estimated from the measured pressure in the gas reservoir. A set of coincidence time spectra between an energy-dispersed electron and a Lyman-α photon is recorded in the multiparameter coincidence system. The electron energy-loss spectrum in coincidence with the detection of Lyman-α photons, simply referred to as the coincident electron energy-loss spectrum, was obtained in the range of an energy loss of 14–43 eV from several sets of time spectra, following almost the same procedure as described in Ref. [36].

III. RESULTS AND DISCUSSION

The ground electronic state of ammonia in C_{3v} symmetry [38] is

$$\tilde{X}\,{}^1A_1\ \underbrace{(1a_1)^2}_{\text{Inner shell}}\ \underbrace{(2a_1)^2}_{\text{Inner valence}}\ \underbrace{(1e)^4(3a_1)^2}_{\text{Outer valence}}.$$

The vertical ionization potentials for the $(3a_1)^{-1}$, $(1e)^{-1}$, $(2a_1)^{-1}$, and $(1a_1)^{-1}$ states of $NH_3{}^+$ are 10.85, 16.4, 27.3, and 405.6 eV, respectively [39,40]. In this article we focus on the energy range of excitation and ionization of valence electrons.

A. Superexcited states of NH_3 associated with the present study

Before showing the experimental results in Fig. 1, we explain below the superexcited states of NH_3 associated with the present study based on the states of $NH_3{}^+$, since ionic states have been studied in more detail than superexcited states of NH_3 [29] and superexcited states are built on ion-core states such that one electron is bound on an ion.

According to the precise calculation of the electronic states of $NH_3{}^+$ by the symmetry-adapted cluster configuration interaction general-R method [41], the $(3a_1)^{-1}$ and $(1e)^{-1}$ states are single-hole states, but the $(2a_1)^{-1}$ state is described as a superposition of the single-hole $(2a_1)^{-1}$ configuration and double-hole one-electron configurations, where the contributions of the double-hole one-electron configurations are comparable to or even larger than that of the single-hole $(2a_1)^{-1}$ configuration. The $(2a_1)^{-1}$ state is a multiconfiguration state, and thus in what follows it is referred to as the '$(2a_1)^{-1}$' state. The quotation marks show that it is in fact a multiconfiguration state. The superexcited state built on the $(1e)^{-1}$ core is a singly excited state referred to as the $(1e)^{-1}$(mo) state. The symbol "mo" stands for the molecular orbital. The singly excited $(1e)^{-1}$(mo) state involves just a single configuration of $(1e)^{-1}$(mo). On the other hand, the superexcited state built on the '$(2a_1)^{-1}$' ion core is not a single-configuration state but is expressed as the superposition of the singly excited $(2a_1)^{-1}$(mo′) configuration and doubly excited configurations. The contribution of the doubly excited configurations appears to be comparable to or even larger than the contribution of the singly excited $(2a_1)^{-1}$(mo′) configuration, as in the '$(2a_1)^{-1}$' ion-core state.

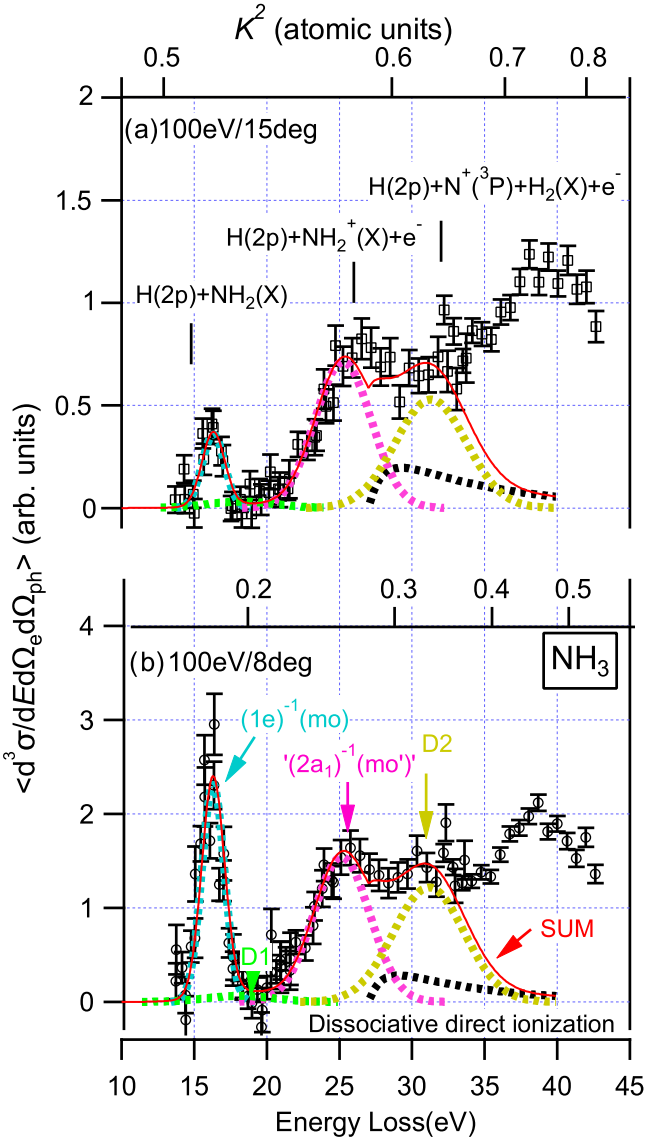

FIG. 1. Electron energy-loss spectra of NH_3 in coincidence with detection of Lyman-α photons measured at 100-eV incident energy and electron scattering angles of (a) 15° and (b) 8°. Differential cross sections are shown on the same relative scale of the vertical axes in (a) and (b). The resolution of the energy loss is approximately 650 meV and the short vertical bars attached to the data points show the statistical uncertainties. Upper axes show the values of K^2, where K is the magnitude of the momentum transfer vector. Long vertical bars show the dissociation limits of the H($2p$) formation indicated. Curves show the results of the fits of Eq. (1) (see the text).

The superexcited state built on the '$(2a_1)^{-1}$' ion core is hence considered a semi–doubly excited state. It is referred to as the '$(2a_1)^{-1}$(mo′)' state. The quotation marks again show that it is in fact a multiconfiguration state. According to Ref. [41], there exist other multiconfiguration states of NH_3^+ ions around the '$(2a_1)^{-1}$' state. Each multiconfiguration state around the '$(2a_1)^{-1}$' state is described as the superposition of some double-hole one-electron configurations with a negligible contribution of single-hole configurations. Superexcited states built on such multiconfiguration states of NH_3^+ ions around the '$(2a_1)^{-1}$' state are hence doubly excited states expressed as the superposition of some doubly excited configurations. The contribution of singly excited configurations appears to be negligible, as in the ion-core states. They are referred to as Dn states, where $n = 1,2,3,\ldots$ is an index used to distinguish ion cores.

The superexcited states of NH_3 mentioned above were substantiated in single-photon absorption and electron collisions of NH_3 by probing with Lyman-α photons in a study by Ishikawa *et al.* [29]. They found four superexcited states of NH_3 that are allowed and result in H($2p$) formation in the range of excitation energy below 32 eV: a singly excited $(1e)^{-1}$(mo) state at an excitation energy of 16.3 eV, a doubly excited $D1$ state at 18.4 eV, a semi–doubly excited '$(2a_1)^{-1}$(mo′)' state at 25.3 eV, and a doubly excited $D2$ state at 31.5 eV. The terms singly and doubly excited states rely on the independent particle model, where the motion of each electron in a many-electron system is described by its own wave function, i.e., orbital. In fact, the doubly excited $D1$ state, semi–doubly excited '$(2a_1)^{-1}$(mo′)' state, and doubly excited $D2$ state are not so amenable to the independent particle model that they are described as the superposition of multiple configurations. On the other hand, the singly excited $(1e)^{-1}$(mo) state is amenable to the independent particle model, and thus it is described with just a single configuration. There is a large difference between the singly excited $(1e)^{-1}$(mo) state and the doubly excited (semi–doubly excited) $D1$, '$(2a_1)^{-1}$(mo′),' and $D2$ states with respect to the validity of the independent particle model. For this reason it is of no significance to distinguish the doubly excited and semi–doubly excited states in this article. In what follows the semi–doubly excited '$(2a_1)^{-1}$(mo′)' state is classified as a doubly excited state.

B. The coincident electron energy-loss spectra

Figures 1(a) and 1(b) show the electron energy-loss spectra of NH_3 in coincidence with detection of Lyman-α photons measured at 100-eV incident energy and at electron scattering angles of 15° and 8°, respectively. The scales of the vertical axes are the same in Figs. 1(a) and 1(b). Several peaks originating from the superexcited states of NH_3 and components of dissociative direct ionizations are observed. These peaks are not seen in the electron energy-loss spectra of NH_3 measured by detecting only energy-dispersed electrons, without any coincidence measurement. The relative contributions of the superexcited states involved change significantly with an increase in the electron scattering angle from just 8° to 15°. It is likely that the allowed superexcited states found by Ishikawa *et al.* [29] contribute to the coincident electron energy-loss spectra in Fig. 1. We obtain the ratios of the differential cross sections due to the doubly excited '$(2a_1)^{-1}$(mo′)' and $D2$ states to the differential cross section due to the singly excited $(1e)^{-1}$(mo) state to substantiate the double-excitation mechanism through the induced electron correlation as mentioned earlier. The $(1e)^{-1}$(mo) state is the singly excited state nearest to the doubly excited $D1$, '$(2a_1)^{-1}$(mo′),' and $D2$ states in terms of energy.

We separate the coincident electron energy-loss spectra in Fig. 1 into the peaks due to precursor superexcited states of

H($2p$) atoms by fitting the equation [29]

$$\frac{d^3\sigma}{dE\,\mathrm{d}\Omega_e d\Omega_{ph}} = \frac{k_s}{k_i}\frac{1}{K^2}\left[\left\{\sum_\alpha A'_\alpha \exp(-B_\alpha(E-E_\alpha)^2)\right\} + \frac{a'}{E}\sigma_{NH_2^+}(E-b)\right], \quad (1)$$

where k_i and k_s are the magnitudes of the wave-number vectors of the incident and scattered electrons, respectively, and K is the magnitude of the momentum transfer vector. The first term on the right-hand side expresses the sum of the contributions of the superexcited states 'α,' and A'_α, B_α, and E_α are constants independent of E. The first term is based on the multidimensional reflection approximation [42] and the semiclassical treatment of the decay dynamics of the superexcited molecules involved [43]. The second term expresses the component of the dissociative direct ionization of $H(2p) + NH_2^+(\tilde{X}) + e^-$, for which the dissociation limit is the lowest among those of the dissociative ionizations resulting in H($2p$) formation [29] and is shown by the vertical bar in Fig. 1. In Eq. (1) $\sigma_{NH_2^+}(E)$ is the cross section of the dissociative direct ionization of $H(1s) + NH_2^+(\tilde{X}) + e^-$ in the photoionization of NH_3 as a function of the incident photon energy E, and a' and b are constants independent of E. Both the energy loss and the incident photon energy express the excitation energy of the target molecule, and thus the same symbol, E, is used for both quantities. We use the cross section of the formation of NH_2^+ in the photoionization of NH_3 measured by Samson *et al.* [44] as $\sigma_{NH_2^+}(E)$. In the range of energy loss above 32.0 eV, there is the possibility that the dissociative ionization of $H(2p) + N^+(^3P) + H_2(X) + e^-$ contributes; its dissociation limit, 32.0 eV, is shown by the vertical bar in Fig. 1 and is the second lowest among the dissociation limits of the dissociative ionizations resulting in H($2p$) formation [29]. We hence fit Eq. (1) to the coincident electron energy-loss spectra in Fig. 1 in the range below 32 eV. The validity of fitting Eq. (1) was described in Ref. [29]. In the fitting, A'_α and a' are fitting parameters, but B_α and E_α for the allowed states mentioned above and b are taken to be the same as those obtained from the cross section for the emission of Lyman-α fluorescence versus the incident photon energy in the single-photon absorption of NH_3 [29] since B_α and E_α are inherent in the superexcited states 'α' and b seems inherent in the process. The resolution of the energy loss, approximately 650 meV, is not taken into account in the fitting of Eq. (1) because the peaks involved in the spectra seem not to be influenced by the resolution. A good fit is obtained throughout the range below 32 eV with the contributions of the singly excited $(1e)^{-1}$(mo) state, the doubly excited $D1$, '$(2a_1)^{-1}$(mo′),' and $D2$ states, and the dissociative direct ionization of $H(2p) + NH_2^+(\tilde{X}) + e^-$ as shown by the dashed and solid curves in Fig. 1: the dashed blue curve represents the $(1e)^{-1}$(mo) state; the dashed pink curve, the '$(2a_1)^{-1}$(mo′)' state; the dashed yellow curve, the $D2$ state; the dashed green curve, the $D1$ state; the dashed black curve, the dissociative direct ionization; and the solid red curve, the sum of the preceding curves. The contribution of the $D1$ state is not noticeable and hence we focus on the singly excited $(1e)^{-1}$(mo) state and doubly excited '$(2a_1)^{-1}$(mo′)' and $D2$ states. The good fit in Fig. 1 obtained with the contributions of only allowed superexcited states shows that the forbidden states make just a small contribution in the range below 32 eV. A forbidden doubly excited state around 35-eV energy loss was recently reported in electron collisions with NH_3 at a 200-eV incident energy and 8° electron scattering angle [45]. However, the contribution of this state seems not to extend to the present fitting range.

C. Domination of dissociative double excitation over dissociative single excitation

As clearly shown in Fig. 1, it is remarkable that the contributions of the dissociative double excitations (dashed pink and yellow curves) become more dominant over that of the nearby dissociative single excitation (dashed blue curve) with a change in the electron scattering angle from just 8° to 15°. The degree of domination is quantitatively shown in terms of the differential cross section $\langle d^2\sigma_\alpha/d\Omega_e d\Omega_{ph}\rangle$, which is obtained from $\langle d^3\sigma_\alpha/dE\,d\Omega_e d\Omega_{ph}\rangle$ using

$$\langle d^2\sigma_\alpha/d\Omega_e d\Omega_{ph}\rangle = \int \langle d^3\sigma_\alpha/dE d\Omega_e d\Omega_{ph}\rangle dE, \quad (2)$$

where $\langle d^3\sigma_\alpha/dE\,d\Omega_e d\Omega_{ph}\rangle$ is the peak due to the superexcited state 'α' in Fig. 1. The quantity $\langle d^2\sigma_\alpha/d\Omega_e d\Omega_{ph}\rangle$ is the differential cross section for the dissociative excitation to the superexcited state 'α' resulting in H($2p$) formation at a given electron scattering angle. The ratio of $\langle d^2\sigma_\alpha/d\Omega_e d\Omega_{ph}\rangle$ to $\langle d^2\sigma_{(1e)^{-1}(mo)}/d\Omega_e d\Omega_{ph}\rangle$ is plotted against the electron scattering angle in Fig. 2 [α = '$(2a_1)^{-1}$(mo′)' and $D2$]. As mentioned the $D2$ and '$(2a_1)^{-1}$(mo′)' states are doubly excited states

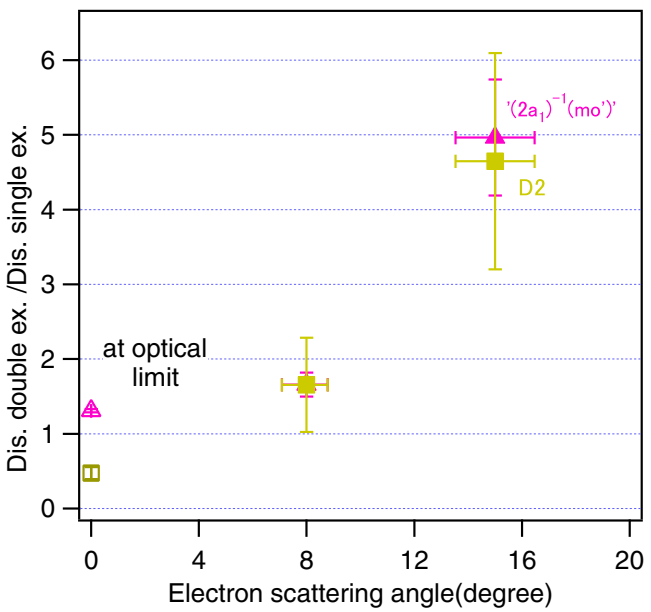

FIG. 2. Ratios of the differential cross sections for dissociative double excitations resulting in H($2p$) formation to that for dissociative single excitation against the electron scattering angle, $\langle d^2\sigma_\alpha/d\Omega_e d\Omega_{ph}\rangle/\langle d^2\sigma_{(1e)^{-1}(mo)}/d\Omega_e d\Omega_{ph}\rangle$ vs the electron scattering angle. Squares, α = the doubly excited $D2$ state; triangles, α = the doubly excited '$(2a_1)^{-1}$(mo′)' state. Open symbols show ratios at the optical limit (see the text). Vertical bars represent errors derived from the uncertainties in fitting Eq. (1), and horizontal bars represent the resolution of the electron scattering angle.

and the $(1e)^{-1}$(mo) state is the singly excited state nearest to them. The angular variation may partly be due to the angular anisotropy of the Lyman-α photons in the averaged differential cross section $\langle d^2\sigma_\alpha/d\Omega_e d\Omega_{ph}\rangle$. However, the angle subtended by the photon detector was so large, i.e., 60°, that the anisotropy of the Lyman-α photons in $\langle d^2\sigma_\alpha/d\Omega_e d\Omega_{ph}\rangle$ was smeared out to a considerable extent. The angular variation seems to be dominated by $\langle d\sigma_\alpha/d\Omega_e\rangle$. It is quantitatively revealed that the dissociative double excitations resulting in H($2p$) formation become more dominant over the dissociative single excitation with increasing electron scattering angle: the ratios increase from 1.5 at 8° up to 5 at 15°. The large increase in the ratios may be attributed to the dynamics and kinematics of electron collisions. The magnitude of the momentum transfer vector, K, plays an important role in the kinematics of electron collisions. As shown on the upper axes in Fig. 1, the value of K^2 ranges from 0.18 to 0.34 a.u. over the region of energy loss where the precursor superexcited states of H($2p$) atoms lie at 8° and from 0.51 to 0.63 a.u. at 15°. The kinematics for excitation to the singly excited $(1e)^{-1}$(mo) state seems approximately the same as that for excitation to the doubly excited '$(2a_1)^{-1}$(mo′)' and $D2$ states at each scattering angle since the value of K^2 does not change quite as much. The remarkable increase in the ratios in Fig. 2—in particular, the ratios much larger than unity at 15°—could not be explained by the kinematics but is mainly attributed to the dynamics of electron collisions. We hence compare the experimental results in Fig. 2 with the aforementioned prediction from the suggested mechanism of double excitation through the electron correlation induced by penetration of the incident electron into the valence orbitals. The suggested mechanism of double excitation is strongly supported by the present experiment since the remarkable increase in the ratios in Fig. 2 is consistent with the prediction.

As mentioned earlier it is reasonable that the induced electron correlation becomes stronger as the electron collision transfers from a distant collision, with a smaller scattering angle, to a close collision, with a larger scattering angle. In this context it is valuable to plot in Fig. 2 the results at an infinite incident energy and a 0° electron scattering angle, i.e., the results at the optical limit, which are derived from the cross section for the emission of Lyman-α fluorescence in the single-photon absorption of NH_3 versus the incident photon energy [29] following the procedure [36] based on the Born-Bethe approximation [27]. The electron collision at the optical limit is an ideal distant collision [46] and does not cause an induced electron correlation. The results at the optical limit again support the suggested mechanism of double excitation through an induced electron correlation since these results are located at the expected position, i.e., a position lower than the data points at 8°.

IV. CONCLUSION

In conclusion, it is found that dissociative double excitation resulting in H($2p$) formation becomes more dominant over dissociative single excitation resulting in H($2p$) formation as the electron collision with NH_3 at 100-eV incident energy transfers from a distant collision (8° scattering angle) to a close collision (15° scattering angle). This remarkable domination is not expected from the independent particle model and strongly supports the double-excitation mechanism through an electron correlation induced by penetration of the incident electron into the valence orbitals of a NH_3 molecule.

[1] M. Imada, A. Fujimori, and Y. Tokura, Rev. Mod. Phys. **70**, 1039 (1998).
[2] Papers in special section on strongly correlated electron systems, J. Phys.: Condens. Matter **24**(29) (2012).
[3] H. Oike, F. Kagawa, N. Ogawa, A. Ueda, H. Mori, M. Kawasaki, and Y. Tokura, Phys. Rev. B **91**, 041101(R) (2015).
[4] J. N. Bardsley, J. Phys. B **1**, 349 (1968).
[5] I. Sánchez and F. Martín, Phys. Rev. A **57**, 1006 (1998).
[6] T. Odagiri *et al.*, J. Phys. B **37**, 3909 (2004).
[7] M. Glass-Maujean *et al.*, J. Phys. B **37**, 2677 (2004).
[8] M. Glass-Maujean and H. Schmoranzer, J. Phys. B **38**, 1093 (2005).
[9] M. Glass-Maujean *et al.*, J. Phys. B **38**, 2871 (2005).
[10] E. M. García *et al.*, J. Phys. B **39**, 205 (2006).
[11] M. Murata *et al.*, J. Phys. B **39**, 1285 (2006).
[12] J. D. Bozek *et al.*, J. Phys. B **39**, 4871 (2006); **41**, 039801 (2008); **42**, 029801 (2009).
[13] J. R. Machacek *et al.*, J. Phys. B **44**, 045201 (2011).
[14] T. Odagiri, Y. Kumagai, M. Nakano, T. Tanabe, I. H. Suzuki, M. Kitajima, and N. Kouchi, Phys. Rev. A **84**, 053401 (2011).
[15] J. E. Furst, T. J. Gay, J. Machacek, D. Kilkoyne, and K. W. McLaughlin, Phys. Rev. A **86**, 041401(R) (2012).
[16] Y. Nakanishi, K. Hosaka, R. Kougo, T. Odagiri, M. Nakano, Y. Kumagai, K. Shiino, M. Kitajima, and N. Kouchi, Phys. Rev. A **90**, 043405 (2014).
[17] K. Hosaka, K. Shiino, Y. Nakanishi, T. Odagiri, M. Kitajima, and N. Kouchi, Phys. Rev. A **93**, 063423 (2016).
[18] L. Ishikawa *et al.*, J. Phys. B **44**, 065203 (2011).
[19] A. Medina *et al.*, J. Phys. B **44**, 215203 (2011).
[20] J. Robert, F. Zappa, C. R. de Carvalho, G. Jalbert, R. F. Nascimento, A. Trimeche, O. Dulieu, A. Medina, C. Carvalho, and N. V. de Castro Faria, Phys. Rev. Lett. **111**, 183203 (2013).
[21] K. Takahashi *et al.*, Eur. Phys. J. D **68**, 83 (2014).
[22] R. Flammini *et al.*, J. Phys. B **33**, 1507 (2000).
[23] A. Lafosse *et al.*, J. Phys. B **36**, 4683 (2003).
[24] F. Martín *et al.*, Science **315**, 629 (2007).
[25] D. Dowek, J. F. Perez-Torres, Y. J. Picard, P. Billaud, C. Elkharrat, J. C. Houver, J. L. Sanz-Vicario, and F. Martin, Phys. Rev. Lett. **104**, 233003 (2010).
[26] A. Fischer *et al.*, J. Phys. B **47**, 021001 (2014).
[27] B. H. Bransden and C. J. Joachain, *Physics of Atoms and Molecules*, 2nd ed. (Pearson Education, London, 2003), pp. 426–427, 705–719.
[28] T. Tsuchida *et al.*, J. Phys. B **44**, 175207 (2011).
[29] L. Ishikawa *et al.*, J. Phys. B **41**, 195204 (2008).

[30] C. G. Ning *et al.*, Chem. Phys. **343**, 19 (2008).
[31] A. O. Bawagan *et al.*, Chem. Phys. **120**, 335 (1988).
[32] C. Plottke *et al.*, J. Phys. B **37**, 3711 (2004).
[33] P. L. Bartlett and A. T. Stelbovics, Phys. Rev. A **81**, 022716 (2010).
[34] J. Wragg and H. W. van der Hart, Phys. Rev. A **94**, 032706 (2016).
[35] T. Nakazato *et al.*, J. Phys. B **40**, 2459 (2007).
[36] K. Yachi *et al.*, J. Phys. B **43**, 155208 (2010).
[37] H. D. Morgan and J. E. Mentall, J. Chem. Phys. **60**, 4734 (1974).
[38] G. Herzberg, *Molecular Spectra and Molecular Structure: III. Electronic Spectra and Electronic Structure of Polyatomic Molecules* (Van Nostrand-Reinhold, Princeton, NJ, 1967), p. 609.
[39] M. N. Piancastelli, C. Cauletti, and M.-Y. Adam, J. Chem. Phys. **87**, 1982 (1987).
[40] M. S. Banna and D. A. Shirley, J. Chem. Phys. **63**, 4759 (1975).
[41] M. Ishida, M. Ehara, and H. Natatsuji, J. Chem. Phys. **116**, 1934 (2002).
[42] R. Schinke, *Photodissociation Dynamics, Cambridge Monographs on Atomic, Molecular and Chemical Physics 1* (Cambridge University Press, Cambridge, UK, 1993), pp. 115–120.
[43] H. Nakamura, J. Phys. Soc. Jpn. **26**, 1473 (1969).
[44] J. A. R. Samson, G. N. Haddad, and L. D. Kilcoyne, J. Chem. Phys. **87**, 6416 (1987).
[45] K. Yamamoto and Y. Sakai, J. Phys. B **45**, 055201 (2012).
[46] C. E. Brion and A. Hamnett, in *Advances in Chemical Physics: The Excited State in Chemical Physics*, Part II, Vol. 45 (John Wiley & Sons, Hoboken, NJ, 1981).